arXiv:cond-mat/0410008v1 [cond-mat.mes-hall] 1 Oct 2004

Spin interferometry with electrons in nanostructures: A road to spintronic devices

U. Zülicke
Institute of Fundamental Sciences, Massey University, Private Bag 11 222, Palmerston North, New Zealand
(Dated: version of 17 July 2004)

The wave nature of electrons in semiconductor nanostructures results in spatial interference effects similar to those exhibited by coherent light. The presence of spin–orbit coupling renders interference in spin space and in real space interdependent, making it possible to manipulate the electron's spin state by addressing its orbital degree of freedom. This suggests the utility of electronic analogs of optical interferometers as blueprints for new spintronics devices. We demonstrate the usefulness of this concept using the Mach–Zehnder interferometer as an example. Its spin–dependent analog realizes a spin–controlled field–effect transistor without magnetic contacts and may be used as a quantum logical gate.

Quantum phase coherence of electrons in nanostructures has been exhibited in a number of interference experiments. Aharonov–Bohm oscillations of the electrical conductance through mesoscopic rings were observed[1,2] and used to design the first solid-state electron interferometers.[3,4] Electronic double–slit[5] and Mach–Zehnder[6] interferometers have recently been realized in two–dimensional (2D) semiconductor heterostructures.[7] In addition to revealing intriguing properties of matter at the nanoscale, quantum–coherence effects could possibly be utilized for the creation of new electronic devices. One example are proposals[8,9] to build quantum switches from coupled electron wave guides.

Recent ideas[10,11] to manipulate current flow by addressing the spin degree of freedom of charge carriers are attracting a lot of interest. Some of these proposals involve phase–coherent spin–dependent transport in nanostructures. Spin dependence can be introduced by the presence of magnetic materials, as in the spin–dependent Fabry–Pérot interferometer[12,13] realized with electrons in magnetic multilayers. Similarly, an early theoretical suggestion[14] for an electronic analog of the electro–optical modulator utilized magnetic contacts as polarizers and analyzers. However, its basic functionality rests on the experimentally confirmed[15,16,17] tunability of spin precession due to the Rashba effect[18] that arises from structural inversion asymmetry[19] in 2D electron systems. As a possible alternative to an entirely magnet–based spintronics, theoretical proposals for spin polarizers without magnets have been put forward recently which are based on the interplay of the Rashba effect with resonant tunneling[20,21,22,23] and quantum interference.[24,25,26] Here we explore a new direction toward spintronics devices that are inspired by quantum–optics setups and combine interferometry in real space with spin precession in nonmagnetic nanostructures.

As an example, we consider the geometry of an electronic Mach–Zehnder (MZ) interferometer shown in Fig. 1. The setup is analogous to its quantum–optics counterpart.[27] Two electronic beam splitters and perfectly reflecting 'mirrors' can be realized in a suitably nanostructured 2D electron systems,[6,28,29] e.g., by point contacts and a hard–wall confinement. To be specific, we assume the interferometer arms to be quasi–onedimensional electron wave guides and characterize beam splitters and mirrors by appropriate scattering matrices.[30] Spin–dependent quantum input and output amplitudes are labeled according to Fig. 1. In addition, front and back gates are used to independently manipulate Rashba spin splitting and electron density in the 2D electron system.[31] In the following, we neglect electron–electron interactions and assume low enough temperature such that the phase–coherence length exceeds the interferometer size.

We first illustrate the basic function of the spin–dependent MZ interferometer by considering the ideal case where the width of electron wave guides is much smaller than the spin–orbit–induced spin precession length L_{so}, and only the lowest wave–guide subband is occupied. To a good approximation, single–electron eigenstates are then also eigenstates of the spin component that is perpendicular to the wave guide and lies in the plane of the 2D electron system. For a given energy E, eigenstates labeled by $=$ have wave numbers

$$k = k_E \frac{}{L_{so}} \text{ where } k_E = \sqrt{\frac{2m E}{h^2} + \left(\frac{}{L_{so}}\right)^2} : \quad (1)$$

The requirement of mutually perpendicular propagation direction and spin–quantization axis for eigenstates results in unavoidable spin mixing at beam splitters and mirrors. In addition, the two eigenstates acquire different dynamical phases

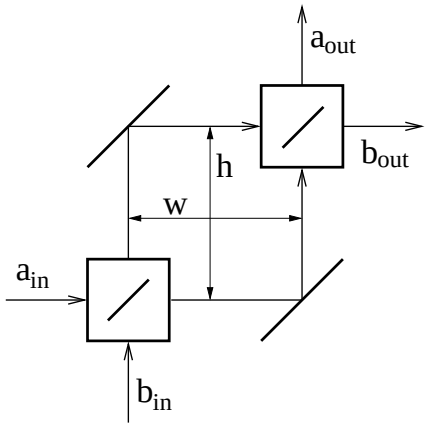


FIG. 1: Schematic setup of the spin–dependent electronic Mach–Zehnder interferometer. Two incident electron spinors, denoted as $a_{in} = (a_{in+}; a_{in-})^T$ and $b_{in} = (b_{in+}; b_{in-})^T$, are mixed by a beam splitter and fed into two interferometer arms. Externally tunable Rashba spin splitting induces spin–dependent dynamical phase shifts for traveling electron waves. The interplay between spin precession during propagation and interference at the second beam splitter determines the output spinor amplitudes a_{out}, b_{out}.

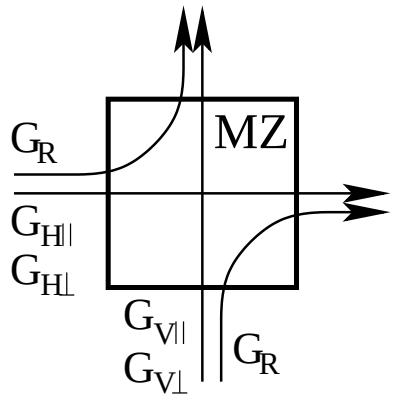


FIG. 2: Transport coefficients for the spin–dependent MZ interferometer, given in the basis of spin–split eigenstates in each lead. Reflection processes are described by a spin–independent conductance G_R. In contrast, horizontal transmission depends on whether spin is conserved (G_{Hk}) or flipped ($G_{H?}$). The same holds for vertical transmission. All conductances can be modulated by gate voltages.

during propagation in the same interferometer arm. Interference effects in the structure are most conveniently embodied in an effective spin–resolved scattering matrix[32] S, relating output spinors a_{out}, b_{out} to the incident ones a_{in}, b_{in}:

$$\begin{pmatrix} a_{out+} \\ a_{out-} \\ b_{out+} \\ b_{out-} \end{pmatrix} = \underbrace{\begin{pmatrix} r_{1++} & r_{1+-} & t_{2++} & t_{2+-} \\ r_{1-+} & r_{1--} & t_{2-+} & t_{2--} \\ t_{1++} & t_{1+-} & r_{2++} & r_{2+-} \\ t_{1-+} & t_{1--} & r_{2-+} & r_{2--} \end{pmatrix}}_{S} \begin{pmatrix} a_{in+} \\ a_{in-} \\ b_{in+} \\ b_{in-} \end{pmatrix} : \tag{2}$$

It can be calculated from the individual scattering matrices for the beam splitters (S_{bs}) and mirrors (S_m). These are[33]

$$S_{bs} = \begin{pmatrix} \frac{i}{2} & \frac{1}{2} & \frac{1}{\sqrt{2}} & 0 \\ \frac{1}{2} & \frac{i}{2} & 0 & \frac{1}{\sqrt{2}} \\ \frac{1}{\sqrt{2}} & 0 & \frac{i}{2} & \frac{1}{2} \\ 0 & \frac{1}{\sqrt{2}} & \frac{1}{2} & \frac{i}{2} \end{pmatrix} ; S_m = \frac{1}{\sqrt{2}} \begin{pmatrix} 0 & i & 1 & 0 \\ 1 & 0 & 0 & i \\ 0 & i & 1 & 0 \\ 0 & 0 & i & 1 \end{pmatrix} ; \tag{3}$$

where the optimal case of identical and symmetric beam splitters is assumed. A standard calculation yields $S = e^{ik_E(h+w)} S^{(MZ)}$ with the energy dependence entirely contained in k_E. $S^{(MZ)}$ has reflection and transmission amplitudes

$$r_{j\,0}^{(MZ)} = i r_{1}^{(MZ)} = i r_{2}^{(MZ)} = \frac{\sin\frac{h}{L_{so}} \sin\frac{w}{L_{so}}}{\sqrt{2}} ; \tag{4a}$$

$$t_{2++}^{(MZ)} = \left[t_{2}^{(MZ)} \right]^{*} = e^{i\frac{h}{L_{so}}} \cos\frac{w}{L_{so}} ; \tag{4b}$$

$$t_{1++}^{(MZ)} = \left[t_{1}^{(MZ)} \right]^{*} = e^{i\frac{w}{L_{so}}} \cos\frac{h}{L_{so}} ; \tag{4c}$$

$$t_{2+-}^{(MZ)} = t_{2-+}^{(MZ)} = \sin\frac{w}{L_{so}} \cos\frac{h}{L_{so}} ; \tag{4d}$$

$$t_{1+-}^{(MZ)} = t_{1-+}^{(MZ)} = \sin\frac{h}{L_{so}} \cos\frac{w}{L_{so}} : \tag{4e}$$

An important functional aspect of the spin MZ interferometer can be gleaned from the linear 4×4 conductance matrix G that is related to the scattering matrix via $G_{jk} = \frac{e^2}{2h} |S_{jk}|^2$. It has a surprisingly simple form:

$$G = \begin{pmatrix} G_R & G_R & G_{Vk} & G_{V?} \\ G_R & G_R & G_{V?} & G_{Vk} \\ G_{Hk} & G_{H?} & G_R & G_R \\ G_{H?} & G_{Hk} & G_R & G_R \end{pmatrix} ; \tag{5}$$

and we find from the results given in Eqs. (4)

$$G_R = \frac{1}{8} \left[1 - \cos\frac{2w}{L_{so}} \right] \left[1 - \cos\frac{2h}{L_{so}} \right] ; \tag{6a}$$

$$G_{Vk} = \frac{1}{2} \left[1 + \cos\frac{2w}{L_{so}} \right] ; \tag{6b}$$

$$G_{Hk} = \frac{1}{2} \left[1 + \cos\frac{2h}{L_{so}} \right] ; \tag{6c}$$

$$G_{V?} = \frac{1}{4} \left[1 - \cos\frac{2w}{L_{so}} \right] \left[1 + \cos\frac{2h}{L_{so}} \right] ; \tag{6d}$$

$$G_{H?} = \frac{1}{4} \left[1 + \cos\frac{2w}{L_{so}} \right] \left[1 - \cos\frac{2h}{L_{so}} \right] : \tag{6e}$$

The physical meaning of these conductances can be understood in terms of probabilities for associated reflection and transmission processes, as illustrated in Fig. 2. Interestingly, reflection processes turn out to be characterized by a spin–rotationally invariant effective conductance G_R. In contrast, transmission probabilities depend on whether or not the spin state is conserved. Spin–conserving transmission depends only on the interferometer size in propagation direction and is different, in general, from transmission involving a spin flip. All conductance coefficients oscillate as functions of the spin–precession length. In addition to general sum rules that are mandated by current conservation,[30] they obey the relation

$$2G_R = \frac{G_{V?}\, G_{H?}}{G_{Vk} G_{Hk}} : \tag{7}$$

Within the single–subband approximation considered here, conductance coefficients are independent of electron energy. This is the same property that the ideal spin field–effect transistor suggested byDatta and Das[14] exhibits. Hence all electrons that are injected into the spin–dependent MZ interferometer within a particular energy window opened by a finite bias voltage will be scattered in an identical manner.

While knowledge of the general conductance coefficients given above allows us to predict transport for interferometers of any size, it is useful to highlight a few special cases. (i) When both w and h are integer multiples of the spin–precession length L_{so}, transmission through the MZ interferometer is perfect, and the vertical and horizontal channels are completely decoupled. Spin–split eigenstates acquire phase factors depending on their wave–number difference and the interferometer size in propagation direction. In other words, the interferometer acts as if it were not there. (ii) When h is an integer multiple of L_{so} and w a half–integer multiple, transmission is still perfect but incurs a spin flip in the vertical

channel. This is true independent of the actual spin state of electrons that are injected into the interferometer. For symmetry reasons, an analogous reflectionless case exists for h and w being half–integer and integer multiples of L_{so}, respectively; but then the spin flip occurs in the horizontal channel. (iii) A purely reflecting case is realized when both h and w are half–integer multiples of L_{so}. The spin of incoming electrons turns out to be conserved in this reflection process. Hence electrons incident in an eigenstate cannot be in an eigenstate after reflection, and their spin will start precessing.

Clearly a suitably designed structure would enable switching between any two cases discussed above by adjusting the spin–precession length. For example, in a MZ interferometer with h = w, there would be two voltages realizing cases (i) and (iii), respectively. As function of one input channel only, such a device acts as a voltage–controlled switch or spin field–effect transistor, similar to the one discussed in Ref.14. As opposed to the design by Datta and Das, however, no magnetic contacts are involved in the present setup, which is somewhat related to the spin interference device proposed in Ref.24. In fact, while spin–dependent interference is crucial for the possibility to switch between perfect transmission and reflection, its effect on the incoming electron beam is the same for any polarization, in particular also for an unpolarized beam.

Changing from case (i) to (ii) would be possible in an interferometer having h = 2w. In that mode, the MZ interferometer acts like a quantum negator for the channel that is transmitted through the shorter interferometer arm. Interestingly, this function is not simply performed here by a Rashba–induced spin precession that was suggested earlier[34,35] as a means to induce phase shifts in a qubit. This is clearly illustrated by the fact that the quantum negation in our MZ interferometer occurs for electrons incident in any spin state, in particular, in Rashba *eigenstates* that would not precess in the previously discussed[35] two–terminal device.

As a further application, the spin–dependent MZ interferometer would be an excellent tool for measuring the effect of any two–terminal device on carrier spin. Such a device could be inserted into one of the interferometer arms, and changes in the output conductances would directly reflect any spin flip or rotation rendered by that device. This would be analogous to the common use of optical MZ interferometers for measuring, e.g., the refractive index of unknown materials.

The the above–discussed functions of the spin–dependent MZ interferometer are independent of electron energy, rendering it unnecessary to keep the electron density constant when tuning spin splitting. Also, multi–subband devices can be expected to work just as well as the single–subband case discussed here, as long as the width of the quasi–onedimensional interferometer arms is smaller than L_{so}. Realization of the suggested spin–dependent MZ interferometer ultimately rests with the possibility to achieve electrostatic control of quantum interference. Recent observation of the electromagnetic Aharonov–Bohm effect,[36] measurement of voltage–controlled conductance modulation in an electronic MZ interferometer[6] and, in particular, demonstration of gate–controlled spin–orbit quantum interference effects in lateral transport[37] suggest that the associated experimental challenges can be met.

In conclusion, we have calculated transport properties of a spin–dependent electronic Mach–Zehnder interferometer. The interplay of electron–wave interference and Rashba spin splitting results in a host of interesting electronic–transport effects. In particular, this structure can work as a field–effect switch. While the device operation is based on spin–dependent interference effects, switching occurs independently of the spin polarization of charge carriers and in the absence of magnetic fields. Certain realizations of such an interferometer perform quantum–logic gate functions. This example leads us to believe that electronic analogs of other optical interferometers in nanostructures with Rashba spin splitting will also lead to interesting new spintronics devices with possible application in quantum–information processing.

[1] R. A. Webb, S. Washburn, C. P. Umbach, and R. B. Laibowitz, Phys. Rev. Lett. **54**, 2696 (1985).
[2] G. Timp et al., Phys. Rev. Lett. **58**, 2824 (1987).
[3] B. J. van Wees et al., Phys. Rev. Lett. **62**, 2523 (1989).
[4] P. G. N. de Vegvar et al., Phys. Rev. B **40**, 3491 (1989).
[5] A. Yacoby et al., Phys. Rev. Lett. **73**, 3149 (1994).
[6] Y. Ji et al., Nature (London) **422**, 415 (2003).
[7] T. Ando, A. B. Fowler, and F. Stern, Rev. Mod. Phys. **54**, 437 (1982).
[8] J. A. del Alamo and C. C. Eugster, Appl. Phys. Lett. **56**, 78 (1990).
[9] C. C. Eugster, J. A. del Alamo, M. J. Rooks, and M. R. Melloch, Appl. Phys. Lett. **64**, 3157 (1994).
[10] S. A. Wolf et al., Science **294**, 1488 (2001).
[11] D. Awschalom, N. Samarth, and D. Loss, eds., *Semiconductor Spintronics and Quantum Computation* (Springer Verlag, Berlin, 2002).
[12] S. Egger, C. H. Back, J. Krewer, and D. Pescia, Phys. Rev. Lett. **83**, 2833 (1999).
[13] S. Egger, C. H. Back, and D. Pescia, J. Appl. Phys. **87**, 7142 (2000).
[14] S. Datta and B. Das, Appl. Phys. Lett. **56**, 665 (1990).
[15] J. Nitta, T. Akazaki, H. Takayanagi, and T. Enoki, Phys. Rev. Lett. **78**, 1335 (1997).
[16] G. Engels, J. Lange, T. Schäpers, and H. Lüth, Phys. Rev. B **55**, R1958 (1997).
[17] Y. Sato, T. Kita, S. Gozu, and S. Yamada, J. Appl. Phys. **89**, 8017 (2001).
[18] Y. A. Bychkov and E. I. Rashba, J. Phys. C **17**, 6039 (1984).
[19] R. Winkler, Phys. Rev. B **62**, 4245 (2000).
[20] E. A. de Andrada e Silva and G. C. La Rocca, Phys. Rev. B **59**, R15583 (1999).
[21] A. A. Kiselev and K. W. Kim, Appl. Phys. Lett. **78**, 775 (2001).
[22] T. Koga, J. Nitta, H. Takayanagi, and S. Datta, Phys. Rev. Lett. **88**, 126601 (2002).
[23] M. Governale, D. Boese, U. Zülicke, and C. Schroll, Phys. Rev. B **65**, 140403(R) (2002).
[24] J. Nitta, F. E. Meijer, and H. Takayanagi, Appl. Phys. Lett. **75**, 695 (1999).
[25] R. Ionicioiu and I. D'Amico, Phys. Rev. B **67**, 041307(R) (2003).
[26] A. A. Kiselev and K. W. Kim, J. Appl. Phys. **94**, 4001 (2003).

[27] R. Loudon, *The Quantum Theory of Light* (Oxford University Press, Oxford, UK, 2000), 3rd ed.
[28] W. D. Oliver, J. Kim, R. C. Liu, and Y. Yamamoto, Science **284**, 299 (1999).
[29] M. Henny et al., Science **284**, 296 (1999).
[30] S. Datta, *Electron Transport in Mesoscopic Systems* (Cambridge University Press, Cambridge, UK, 1995).
[31] S. J. Papadakis et al., Science **283**, 2056 (1999).
[32] T. P. Pareek, Phys. Rev. Lett. **92**, 076601 (2004).
[33] G. Feve, W. D. Oliver, M. Aranzana, and Y. Yamamoto, Phys. Rev. B **66**, 155328 (2002).
[34] J. C. Egues, G. Burkard, and D. Loss, Phys. Rev. Lett. **89**, 176401 (2002).
[35] A. E. Popescu and R. Ionicioiu, Phys. Rev. B **69**, 245422 (2004).
[36] W. G. van der Wiel et al., Phys. Rev. B **67**, 033307 (2003).
[37] J. B. Miller et al., Phys. Rev. Lett. **90**, 076807 (2003).